J. Am. Soc. Mass Spectrom. (2013)
DOI: 10.1007/s13361-013-0636-7

RESEARCH ARTICLE

Minimization of Fragmentation and Aggregation by Laser Desorption Laser Ionization Mass Spectrometry

Qinghao Wu,[1] Andrew E. Pomerantz,[2] Oliver C. Mullins,[2] Richard N. Zare[1]

[1]Department of Chemistry, Stanford University, Stanford, CA 94305-5080, USA
[2]Schlumberger-Doll Research Center, 1 Hampshire St., Cambridge, MA 02139, USA

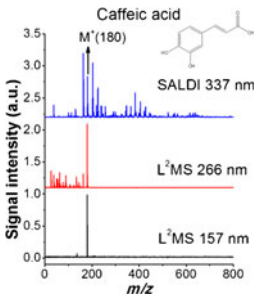

Abstract. Measuring average quantities in complex mixtures can be challenging for mass spectrometry, as it requires ionization and detection with nearly equivalent cross-section for all components, minimal matrix effect, and suppressed signal from fragments and aggregates. Fragments and aggregates are particularly troublesome for complex mixtures, where they can be incorrectly assigned as parent ions. Here we study fragmentation and aggregation in six aromatic model compounds as well as petroleum asphaltenes (a naturally occurring complex mixture) using two laser-based ionization techniques: surface assisted laser desorption ionization (SALDI), in which a single laser desorbs and ionizes solid analytes; and laser ionization laser desorption mass spectrometry (L^2MS), in which desorption and ionization are separated spatially and temporally with independent lasers. Model compounds studied include molecules commonly used as matrices in single laser ionization techniques such as matrix assisted laser desorption ionization (MALDI). We find significant fragmentation and aggregation in SALDI, such that individual fragment and aggregate peaks are typically more intense than the parent peak. These fragment and aggregate peaks are expected in MALDI experiments employing these compounds as matrices. On the other hand, we observe no aggregation and only minimal fragmentation in L^2MS. These results highlight some advantages of L^2MS for analysis of complex mixtures such as asphaltenes.

Key words: SALDI, L^2MS, Laser ionization, Fragmentation, Aggregation

Received: 28 January 2013/Revised: 24 March 2013/Accepted: 2 April 2013

Introduction

Mass spectrometry is a powerful tool for analysis of complex mixtures. Advances in high resolution analysis now permit the identification of thousands of individual components in complex mixtures [1–6]. Moreover, novel techniques are being developed to measure average quantities of complex mixtures [7–9]. This work complements other spectroscopic analyses measuring the abundance of functional groups in mixtures [10–15].

The average molecular weight of a complex mixture is an important quantity and naturally suited for analysis by mass spectrometry. However, polydisperse samples present numerous significant challenges for mass spectrometry: each component must ionize with comparable cross section, and minimal matrix effect, fragmentation, and aggregation must be suppressed or at least moved outside the region where singly-charged parent ions appear, the mass analyzer must have similar sensitivity for all masses, etc. The issue of fragmentation and ionization can be particularly challenging because fragments or aggregates incorrectly assigned as parent ions can lead to large errors in the resulting average molecular weight [9, 16–18]. In spectra of pure compounds or simple mixtures, knowledge of the ionization process can facilitate assignment of spectral peaks as fragments or aggregates, and those peaks can then be removed in the calculation of average molecular weight. For complex mixtures, fragments or aggregates of one component may have a mass similar to the parent mass of another component, complicating the assignment and removal of fragment and aggregate signatures.

Laser-based ionization techniques are often used for analysis of a wide range of samples. The simplest laser-based ionization technique is laser desorption ionization (LDI), which uses a single laser pulse to desorb and ionize

Electronic supplementary material The online version of this article (doi:10.1007/s13361-013-0636-7) contains supplementary material, which is available to authorized users.

Correspondence to: Richard N. Zare; *e-mail:* zare@stanford.edu

Published online: 30 April 2013

analytes simultaneously. A more common technique is matrix-assisted laser desorption/ionization (MALDI) mass spectrometry, in which the analyte is mixed with a matrix to aid in desorption and ionization [19–22]. The presence of a matrix enhances the sensitivity, and MALDI is commonly used for analysis of small molecules either as pure compounds or simple mixtures. Another common technique is surface assisted laser desorption/ionization mass spectrometry (SALDI-MS), in which the modified surface of a sample plate assists in transferring energy to the analyte, resulting in more efficient desorption and ionization [23–27]. A variety of substrates has been investigated, including silicon [23], carbon-based materials [28–31], semiconductors [32, 33], and metals [34–37], and generally good performance is obtained for analysis of small molecules [34, 38]. However, fragmentation and, especially, aggregation can occur in all of these methods, and it has been proposed that aggregation results from ion-induced dipole attractions in the dense cloud of ions [39].

An alternative laser-based ionization technique is laser desorption laser ionization mass spectrometry (L^2MS). Here, desorption and ionization are separated in time and in space and are performed with separate lasers [40–42]. In the desorption step, a pulsed infrared (IR) laser desorbs analytes from the surface of some substrate, such as glass or quartz. In the ionization step, gas-phase analytes are photoionized, typically by either resonant enhanced multiphoton ionization (REMPI) at 266 nm or single-photon ionization (SPI) at 157 nm. REMPI is a selective ionization method, which is advantageous for ionizing compounds containing fused benzene rings, such as polycyclic aromatic hydrocarbons (PAHs). On the other hand, SPI at 157 nm (7.9 eV) is a nearly universal ionization method for compounds with ionization energies lower than this photon energy [43]. A benefit of the two-step process is that ionization occurs in vacuum, where the density is typically too low for ion-induced dipole attractions to cause aggregation. L^2MS has been used in a variety of applications, including ancient terrestrial rocks [44], sediments and soils [45, 46], meteorites [47, 48], interplanetary dust particles [49, 50], stardust [51], atmospheric aerosols [52], agricultural samples [53], polymers [54], asphaltenes [7, 8, 39, 55, 56], and natural water samples [57]. The analytes detected typically include PAHs, heteroatom- and alkyl-substituted PAHs, and porphyrins. In contrast to single laser ionization methods, L^2MS spectra of these compounds do not contain significant signals from aggregates.

Here we compare directly the performance of single-laser and two-laser analyses, and we extend the investigation beyond the compounds that have traditionally been analyzed by two-laser techniques. Single-laser analyses are performed with SALDI, and two-laser analyses are performed with L^2MS involving both REMPI and SPI. Mass spectra are recorded for compounds in five different categories as well as asphaltenes, a complex mixture found in crude oil. The data show that aggregates common in SALDI are nearly eliminated in L^2MS, and that fragments common in SALDI are reduced in REMPI-L^2MS and nearly eliminated in SPI-L^2MS. The results suggest the L^2MS can be an effective ionization technique for analysis of complex mixtures, where aggregates and fragments present in other ionization technique complicate spectral interpretation.

Experimental

Sample Preparation

Compounds in five different categories including a PAH, a nitrile-substituted PAH, two aromatic carboxylic acids, an aromatic amino acid, and a nucleobase were studied. All compounds were purchased from Sigma-Aldrich (St. Louis, MO, USA) and used without further purification. Asphaltene molecules were extracted from Middle Eastern crude oils by diluting the crude oil 1:40 in *n*-heptane and waiting 2 d for the asphaltenes to precipitate. The asphaltenes were extracted from the solution by vacuum filtration through a nylon membrane possessing 0.65-μm pores. The asphaltenes were then dried and dissolved in toluene to eliminate any non-asphaltene species in the crude oil that are insoluble in *n*-heptane (typically inorganic species). The solution of asphaltenes in toluene was diluted in *n*-heptane and vacuum filtered as before. Finally, the asphaltenes were washed by Soxhlet extraction in *n*-heptane for 2 d.

Prior to introduction into the mass spectrometer, the model compounds are dissolved in either toluene or in an ethanol/water mixture (1:1) to form a solution of 2.5 mmol/L, and the asphaltenes are dissolved in toluene to form a solution of 2 mg/mL. In the SALDI experiments, approximately 4 μL of solution is deposited on an NP20 array, which is a commercial silicon group modified substrate (Ciphergen, Fremont, CA, USA). The array was fixed on a cassette and loaded into a high vacuum, after allowing 15–30 min for the solvent to evaporate under ambient conditions. In the L^2MS experiments, small crystals of the model compounds are fixed on a copper platter with double-sided tape (Scotch 3M) and transferred into the vacuum chamber through an interlock. No significant signal was observed from the use of double-sided tape alone. In the case of asphaltene analysis, a 20-μL drop of the asphaltene solution was spotted onto a glass platter and dried under ambient conditions before being introduced into the system.

Surface Assisted Laser Desorption/Ionization Mass Spectrometry

SALDI-TOF mass spectra were obtained using a PCS4000 mass spectrometer (Bio-Rad, Fremont, CA, USA). Nonselective normal phase NP20 arrays (Ciphergen, Fremont, CA, USA) were used. The surface of the arrays was modified by the addition of silicon oxide groups. Mass spectra were acquired using a pulsed nitrogen laser with a wavelength of 337 nm. The laser pulse energy was varied from 250 to 2000 nJ in steps of 250 nJ for each compound. The mass spectra were externally calibrated using a standard

mixture of low molecular weight peptides (Bio-Rad). Data were acquired in the positive ion mode from *m/z* 0 to 10,000, focused at 200 Da.

Two-step Laser Desorption Laser Ionization Mass Spectrometry

The L^2MS technique has been described in detail elsewhere [42, 55, 58, 59], and this section provides a brief description of the apparatus. The sample is introduced into a high-vacuum chamber through a vacuum interlock and positioned under the extraction region of the mass spectrometer. The sample is allowed to outgas for ~30 min to reduce the background signal after being positioned. A pulse of infrared (IR) light from a CO_2 laser (λ=10.6 μm; Alltec GmbH, Selmsdorf, Germany, model AL 882 APS) is focused to a spot (~50 μm in diameter) on the sample surface using a Cassegrainian microscope objective (Ealing Optics, San Jose, CA, USA, 15×). This IR laser pulse can generate a heating rate of about 10^8 K/s on the highly localized area [40], which desorbs molecules from the surface of the glass platter. This rapid heating process favors desorption over decomposition, allowing this technique to desorb neutral species with minimal fragmentation.

Desorbed neutral molecules from the platter surface form a plume in the extraction region during a time of 10 to 50 μs. This plume is intersected perpendicularly by the VUV output of the fourth harmonic (λ=266 nm) of a Nd:YAG laser (Spectra Physics, Santa Clara, CA, USA, DCR 11) or a pulsed F_2 excimer laser (λ=157 nm; Coherent, Inc., Santa Clara, CA, USA, ExciStar XS 200). The 266-nm laser pulse ionizes desorbed molecules through 1+1 resonance enhanced multiphoton ionization (REMPI) with combined photon energy of 9.3 eV. This ionization method is suitable for ionizing organic species that absorb around 266 nm; thus, it is a selective ionization method for PAHs or PAH-substituted molecules. The photon fluence for the 266 nm laser is about 10 mJ/cm^2. Different from REMPI, the SPI is a nearly universal ionization technique for any molecule with an ionization potential below the photon energy of 7.89 eV, which is sufficient for ionizing aromatic species. The photon fluence is approximately 5 mJ/cm^2.

The created ions are mass analyzed in a homebuilt reflectron time-of-flight mass spectrometer (TOF-MS) employing a modified Wiley–McLaren geometry. A dual microchannel plate set in a Chevron configuration (MCPs; 20 cm^2 active area; Burle Electro-Optics, Sturbridge, MA, USA) coupled to a large collector anode (Galileo TOF-4000) is used as a detector. The generated ion signal is amplified by a fast pre-amplifier (Ortec 9326) and a timing filter (Ortec 474), after which it is displayed on a digital oscilloscope (LeCroy 9450). Each recorded spectrum is averaged over 30 laser shots. The mass resolution of this instrument is approximately one mass unit at *m/z* 500, which is comparable to the resolution of SALDI instrument.

Limits of Detection

Limits of detection (LODs) in L^2MS are influenced by a variety of parameters, such as the delay time between the two lasers, voltage optimization for the mass analyzer, and the laser pulse energies in both IR and UV lasers [60]. LODs (S/N=3) for coronene are evaluated to be 50 nmol/mm^2 in normal operation conditions. In SALDI, the LODs are mainly influenced by the laser pulse energy. At the laser pulse energy of 500 nJ, the LODs for coronene are evaluated to be 0.6 nmol/mm^2. Even better results can be obtained by optimizing the conditions. It is believed that the higher LODs in the L^2MS are mainly caused by the loss in the laser desorption step, in which most neutral molecules were scattered away from the ionization region.

Results and Discussion

The Effect of Laser Power

The laser pulse energy in SALDI has a remarkable influence on the mass spectra. With more laser pulse energy, fragmentation and aggregation of ions significantly increased (Figure 1). It is believed that more energy was transferred into analyte molecules through the substrate and, thus, generates more fragments with increased laser pulse energy. The increased laser pulse energy also generates more charged and neutral particles, which form a denser plasma plume. Accordingly, the possibility of aggregation in the denser plasma rises because of the increased frequency of collisions. Therefore, fragmentation and aggregation between fragment ions, molecules, and metal atoms/ions from substrate increased more significantly than the parent ions when the laser pulse energy increased.

In L^2MS experiments, results have shown that the IR laser pulse energy influences the signal intensity rather than the aggregation, suggesting separated molecules are desorbed from the aggregated solid phase [8, 56, 60]. In

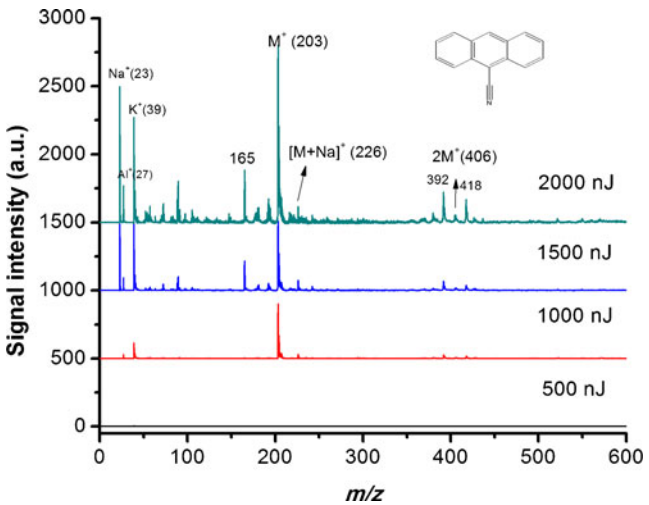

Figure 1. The mass spectra obtained with different laser powers in SALDI

the ionization step, the molecules may be decomposed into fragments by absorbing more photons in a very intense laser pulse, but this situation can be easily avoided with a proper UV laser pulse energy.

Due to the importance of laser pulse energies in both SALDI and L^2MS, they were carefully optimized before each experiment. The laser pulse energy in SALDI was studied from 500 to 2000 nJ in step of 250 nJ for each compound. Mass spectra with reasonable signal level but less fragmentations and aggregations were chosen to compare with mass spectra in L^2MS, in which both IR and UV laser pulses were optimized separately. As Figure 1 shows, there is a threshold pulse energy below which no detectable SALDI signal is found. SALDI mass spectra were acquired with a pulse energy just above threshold and at higher values. The optimization in L^2MS was mainly based on the signal intensity rather than pattern of the mass spectrum because fragmentation and aggregation are rare. Mass spectra presented below were acquired with optimized results in SALDI and L^2MS.

Mass Spectra of Non-Fragile Compounds

Figure 2 compares the mass spectra of coronene from SALDI (337-nm pulse) with that of L^2MS with both 226-nm and 157-nm laser pulses. All mass spectra show a dominant parent ion at m/z 300, demonstrating that each technique can achieve soft ionization under favorable conditions. Despite the fact that the photon energy in SALDI is much less than that in L^2MS, the fragment ion signal at m/z=276 in SALDI is much stronger than that in both spectra of L^2MS, suggesting that molecules in SALDI absorbed more energy than in L^2MS. The dimer ions at m/z=600 and fragment attached parent ions at m/z=374 indicate aggregation in SALDI. In addition, more multimers were observed with increased laser pulse energy in our experiments (data not shown), which is consistent with the findings of others [9]. In sharp contrast, both spectra in L^2MS are very clean: no aggregates are observed; no fragment ions are detected in 157-nm pulsed laser ionization; instead, only a small amount of fragment ions at m/z=276 and 40 appear from the REMPI-L^2MS. Similar results can also be found in the spectra of 9-anthracenecarbonitrile (Supporting Information, Figure S-1).

For the non-fragile compounds, both of SALDI and L^2MS show the capability of soft ionization with little fragments. Most fragments and aggregated ions in SALDI are easy to assign. In L^2MS, the aggregated ions are below LODs. Fragments in L^2MS are weak for REMPI and nearly eliminated for SPI.

Mass Spectra of Fragile Compounds

Fragments from fragile compounds such as carboxylic acids, amino acid, and aminobases are easily formed by breaking bonds between functional groups and other parts of molecule. Also, aggregation is expected from dipole–dipole attractions between polar groups in different molecules. The molecules 2,5-dihydroxybenzoic acid, caffeic acid, L-tryptophan, and 2,6-diaminopurine were selected.

The mass spectrum of caffeic acid in SALDI shows intense fragments and alkali metal attached ions (Figure 3a). An intense fragment at m/z=163 in the SALDI spectrum indicates that OH is easily lost in the ionization. The Na, K, and COOH attached ions at m/z=203, 219, and 225 suggest that the metallic and fragment ion attachment in the SALDI are one of the main ionization methods. On the contrary, no aggregation is found in L^2MS and the parent ions are dominant. A series of fragments in REMPI-L^2MS are found

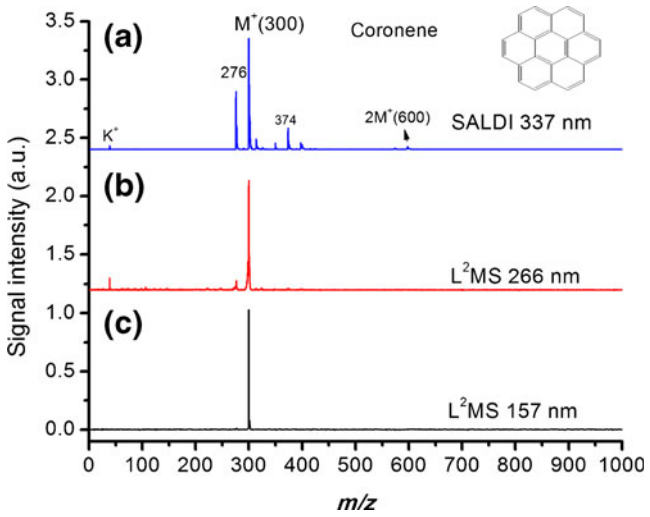

Figure 2. The mass spectra of coronene in (**a**) SALDI with 337-nm ionization, (**b**) L^2MS with 266-nm REMPI, and (**c**) L^2MS with 157-nm SPI

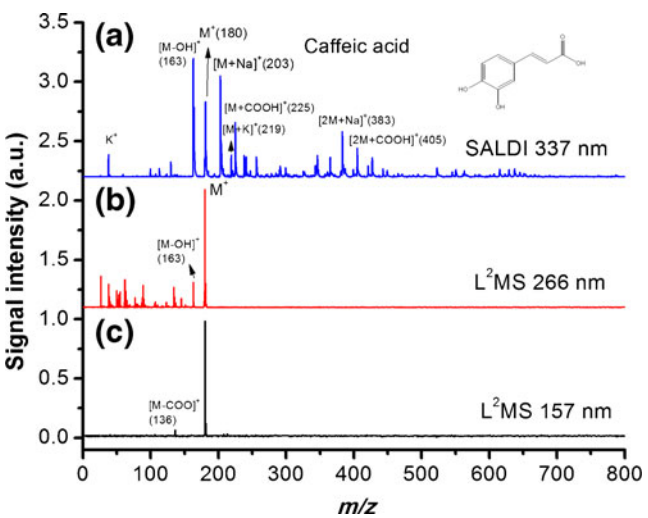

Figure 3. The mass spectra of caffeic acid in (**a**) SALDI with 337-nm ionization, (**b**) L^2MS with 266-nm REMPI, and (**c**) L^2MS with 157-nm SPI

(Figure 3b), but only a small fragment at m/z=136 appeared in the spectrum of SPI-L^{2}MS (Figure 3c).

The SALDI mass spectrum of L-tryptophan includes a variety of peaks, such as the parent ions, Na attached parent ions, metal ions from the substrate, fragment ions, and unidentified aggregated ions (Figure 4a). These peaks form a complex mass spectrum. On the other hand, in L^{2}MS, no aggregates are found again. The fragment at m/z=130 is dominant in REMPI-L^{2}MS (Figure 4b), but very weak in SPI-L^{2}MS (Figure 4c). The mass spectra of both 2,5-dihydroxybenzoic acid and 2,6-diaminopurine also show similar mass spectra: weak parent ions and intense fragments and aggregates in SALDI; less fragments and no aggregates in L^{2}MS (Supplementary information, Figures S-2 and S-3).

Generally, the mass spectra of these polar and fragile compounds in SALDI show complex spectrum with intensive fragmentation and aggregation, which is difficult to interpret. Fragment and aggregate peaks are more intense than the parent ions in all compounds studies. On the other hand, no aggregates are observed in L^{2}MS. Fragment ions are weak in most of the REMPI-L^{2}MS and negligible in SPI-L^{2}MS.

Mass Spectra of Asphaltene Molecules

The SALDI mass spectra of petroleum asphaltenes have been published previously and indicated the observation of aggregated ions at high laser power and/or sample concentration [16, 61–63]. This signal has been attributed to aggregate formation in the dense plasma during desorption/ionization process. The L^{2}MS mass spectra of petroleum asphaltenes have also been published previously and showed no indication of aggregates signals over the mass range studied (below 2000m/z) [8, 39, 55, 56]. According to the Yen–Mullins model of asphaltene aggregation, asphaltenes can form stable structures near 5000m/z, referred to as nanoaggregates [64, 65]. Figure 5 presents the mass spectra

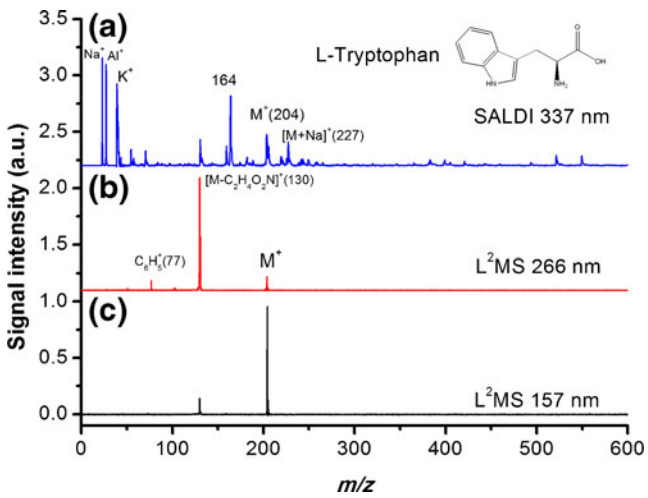

Figure 4. The mass spectra of L-Tryptophan in (**a**) SALDI with 337-nm ionization, (**b**) L^{2}MS with 266-nm REMPI, and (**c**) L^{2}MS with 157-nm SPI

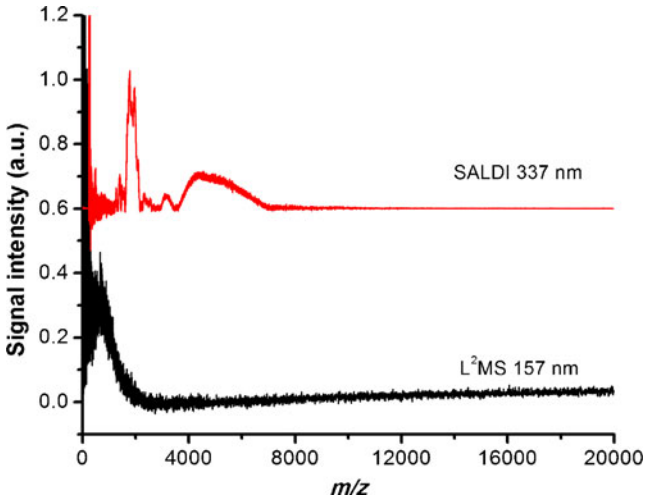

Figure 5. The mass spectra of UG8 asphaltenes in (**a**) SALDI with 337-nm ionization with laser energy of 2500 nJ, and (**b**) L^{2}MS with 157-nm SPI

of UG8 petroleum asphaltene recorded out to 20,000m/z in SALDI and SPI-L^{2}MS. In SPI-L^{2}MS, no aggregates of any form are detected in this molecular weight range, whereas the peak from 1600 to 2100 u and broad peak from 4000 to 7000 u are the evidence of aggregation in SALDI.

Conclusions

Fragmentation and aggregation in SALDI, REMPI-L^{2}MS, and SPI-L^{2}MS have been studied by measuring mass spectra of six model compounds and a naturally occurring petroleum asphaltene sample. Even under optimized conditions, fragmentation and aggregation are extensive in SALDI, and fragment and aggregate signals are often more intense than the parent molecular ion signal. Similar signals can be expected for MALDI experiments, where these compounds are used as matrices. This fragmentation and aggregation complicates interpretation of the mass spectra, especially for small molecules and mixtures where aggregate peaks from one molecule may overlap parent ion peaks from another molecule. In stark contrast, mass spectra acquired with L^{2}MS contain no detectable aggregate peaks. It is suggested that aggregation is minimized in L^{2}MS because the IR laser is sufficient to break noncovalent bonds in the solid sample, resulting in desorption of isolated neutral molecules. The plume of desorbed neutrals lacks ions that cause ion-induced dipole attractive forces leading to aggregation in the gas phase. Fragmentation occurs occasionally in REMPI-L^{2}MS (two photon energy=9.3 eV) and rarely in SPI-L^{2}MS (single photon energy=7.9 eV) for the compounds studied because in the latter case, the photon energy is only slightly above the ionization potential of these molecules. The minimization of fragmentation and aggregation implies that L^{2}MS may be an attractive ionization technique for analysis of complex mixtures, where fragmentation and aggregation found in traditional ionization techniques result in mass spectra that are difficult to interpret.

Acknowledgments

The authors are grateful to John Whitin, School of Medicine, Stanford University, for assistance in SALDI. They thank Hassan Sabbah, Université de Toulouse, for useful discussions.

References

1. Fernandez-Lima, F.A., Becker, C., McKenna, A.M., Rodgers, R.P., Marshall, A.G., Russell, D.H.: Petroleum crude oil characterization by IMS-MS and FTICR MS. *Anal. Chem.* **81**, 9941–9947 (2009)
2. Baidoo, E.E.K., Benket, P.I., Neususs, C., Pelzing, M., Kruppa, G., Leary, J.A., Keasling, J.D.: Capillary electrophoresis-Fourier transform ion cyclotron resonance mass spectrometry for the identification of cationic metabolites via a pH-mediated stacking-transient isotachophoretic method. *Anal. Chem.* **80**, 3112–3122 (2008)
3. Armirotti, A.: Bottom-up proteomics. *Curr. Anal. Chem.* **5**, 116–130 (2009)
4. Durbin, K.R., Tran, J.C., Zamdborg, L., Sweet, S.M.M., Catherman, A.D., Lee, J.E., Li, M.X., Kellie, J.F., Kelleher, N.L.: Intact mass detection, interpretation, and visualization to automate top-down proteomics on a large scale. *Proteomics* **10**, 3589–3597 (2010)
5. Rodgers, R.P., McKenna, A.M.: Petroleum analysis. *Anal. Chem.* **83**, 4665–4687 (2011)
6. Marshall, A.G., Rodgers, R.P.: Petroleomics: Chemistry of the underworld. *Proc. Natl. Acad. Sci. U. S. A.* **105**, 18090–18095 (2008)
7. Sabbah, H., Morrow, A.L., Pomerantz, A.E., Zare, R.N.: Evidence for island structures as the dominant architecture of asphaltenes. *Energy Fuel* **25**, 1597–1604 (2011)
8. Pomerantz, A.E., Hammond, M.R., Morrow, A.L., Mullins, O.C., Zare, R.N.: Asphaltene molecular-mass distribution determined by two-step laser mass spectrometry. *Energy Fuel* **23**, 1162–1168 (2009)
9. Hortal, A.R., Hurtado, P., Martinez-Haya, B., Mullins, O.C.: Molecular-weight distributions of coal and petroleum asphaltenes from laser desorption/ionization experiments. *Energy Fuel* **21**, 2863–2868 (2007)
10. Painter, P.C., Snyder, R.W., Starsinic, M., Coleman, M.M., Kuehn, D.W., Davis, A.: Concerning the application of FT-IR to the study of coal—a critical-assessment of band assignments and the application of spectral-analysis programs. *Appl. Spectrosc.* **35**, 475–485 (1981)
11. George, G.N., Gorbaty, M.L.: Sulfur K-edge X-ray absorption-spectroscopy of petroleum asphaltenes and model compounds. *J. Am. Chem. Soc.* **111**, 3182–3186 (1989)
12. Mitrakirtley, S., Mullins, O.C., Vanelp, J., George, S.J., Chen, J., Cramer, S.P.: Determination of the nitrogen chemical structures in petroleum asphaltenes using xanes spectroscopy. *J. Am. Chem. Soc.* **115**, 252–258 (1993)
13. Kelemen, S.R., Afeworki, M., Gorbaty, M.L., Sansone, M., Kwiatek, P.J., Walters, C.C., Freund, H., Siskin, M., Bence, A.E., Curry, D.J., Solum, M., Pugmire, R.J., Vandenbroucke, M., Leblond, M., Behar, F.: Direct characterization of kerogen by X-ray and solid-state C-13 nuclear magnetic resonance methods. *Energy Fuel* **21**, 1548–1561 (2007)
14. Andrews, A.B., Edwards, J.C., Pomerantz, A.E., Mullins, O.C., Nordlund, D., Norinaga, K.: Comparison of coal-derived and petroleum asphaltenes by C-13 nuclear magnetic resonance, DEPT, and XRS. *Energy Fuel* **25**, 3068–3076 (2011)
15. Solum, M.S., Pugmire, R.J., Grant, D.M.: C-13 solid-state NMR of argonne premium coals. *Energy Fuel* **3**, 187–193 (1989)
16. Hortal, A.R., Martinez-Haya, B., Lobato, M.D., Pedrosa, J.M., Lago, S.: On the determination of molecular weight distributions of asphaltenes and their aggregates in laser desorption ionization experiments. *J. Mass Spectrom.* **41**, 960–968 (2006)
17. Strausz, O.P., Peng, P., Murgich, J.: About the colloidal nature of asphaltenes and the MW of covalent monomeric units. *Energy Fuel* **16**, 809–822 (2002)
18. Domin, M., Li, S., Lazaro, M.J., Herod, A.A., Larsen, J.W., Kandiyoti, R.: Large molecular mass materials in coal-derived liquids by Cf-252-plasma and matrix-assisted laser desorption mass spectrometry. *Energy Fuel* **12**, 485–492 (1998)
19. Karas, M., Hillenkamp, F.: Laser desorption ionization of proteins with molecular masses exceeding 10000 daltons. *Anal. Chem.* **60**, 2299–2301 (1988)
20. Aebersold, R., Mann, M.: Mass spectrometry-based proteomics. *Nature* **422**, 198–207 (2003)
21. Knochenmuss, R., Zenobi, R.: MALDI ionization: The role of in-plume processes. *Chem. Rev.* **103**, 441–452 (2003)
22. Pan, C., Xu, S., Zhou, H., Fu, Y., Ye, M., Zou, H.: Recent developments in methods and technology for analysis of biological samples by MALDI-TOF-MS. *Anal. Bioanal. Chem.* **387**, 193–204 (2007)
23. Wei, J., Buriak, J.M., Siuzdak, G.: Desorption-ionization mass spectrometry on porous silicon. *Nature* **399**, 243–246 (1999)
24. Ha, T.K., Lee, T.G., Song, N.W., Moon, D.W., Han, S.Y.: Cation-assisted laser desorption/ionization for matrix-free surface mass spectrometry of alkanethiolate self-assembled monolayers on gold substrates and nanoparticles. *Anal. Chem.* **80**, 8526–8531 (2008)
25. Guenin, E., Lecouvey, M., Hardouin, J.: Could a nano-assisted laser desorption/ionization target improve the study of small organic molecules by laser desorption/ionization time-of-flight mass spectrometry? *Rapid Commun. Mass Spectrom.* **23**, 1395–1400 (2009)
26. Kailasa, S.K., Wu, H.-F.: Multifunctional ZrO2 nanoparticles and ZrO2-SiO2 nanorods for improved MALDI-MS analysis of cyclodextrins, peptides, and phosphoproteins. *Anal. Bioanal. Chem.* **396**, 1115–1125 (2010)
27. Shen, Z.X., Thomas, J.J., Averbuj, C., Broo, K.M., Engelhard, M., Crowell, J.E., Finn, M.G., Siuzdak, G.: Porous silicon as a versatile platform for laser desorption/ionization mass spectrometry. *Anal. Chem.* **73**, 612–619 (2001)
28. Dattelbaum, A.M., Iyer, S.: Surface-assisted laser desorption/ionization mass spectrometry. *Expert Rev. Proteome.* **3**, 153–161 (2006)
29. Najam-ul-Haq, M., Rainer, M., Szabo, Z., Vallant, R., Huck, C.W., Bonn, G.K.: Role of carbon nano-materials in the analysis of biological materials by laser desorption/ionization-mass spectrometry. *J. Biochem. Biophys. Methods* **70**, 319–328 (2007)
30. Tang, H.-W., Ng, K.-M., Lu, W., Che, C.-M.: Ion desorption efficiency and internal energy transfer in carbon-based surface-assisted laser desorption/ionization mass spectrometry: Desorption mechanism(s) and the design of SALDI substrates. *Anal. Chem.* **81**, 4720–4729 (2009)
31. Zhang, H., Cha, S., Yeung, E.S.: Colloidal graphite-assisted laser desorption/ionization MS and MS^n of small molecules. 2. Direct profiling and MS imaging of small metabolites from fruits. *Anal. Chem.* **79**, 6575–6584 (2007)
32. Lewis, W.G., Shen, Z.X., Finn, M.G., Siuzdak, G.: Desorption/ionization on silicon (DIOS) mass spectrometry: Background and applications. *Int. J. Mass Spectrom.* **226**, 107–116 (2003)
33. Northen, T.R., Woo, H.-K., Northen, M.T., Nordstroem, A., Uritboonthail, W., Turner, K.L., Siuzdak, G.: High surface area of porous silicon drives desorption of intact molecules. *J. Am. Soc. Mass Spectrom.* **18**, 1945–1949 (2007)
34. Law, K.P., Larkin, J.R.: Recent advances in SALDI-MS techniques and their chemical and bioanalytical applications. *Anal. Bioanal. Chem.* **399**, 2597–2622 (2011)
35. Kruse, R.A., Li, X.L., Bohn, P.W., Sweedler, J.V.: Experimental factors controlling analyte ion generation in laser desorption/ionization mass spectrometry on porous silicon. *Anal. Chem.* **73**, 3639–3645 (2001)
36. Piret, G., Coffinier, Y., Roux, C., Melnyk, O., Boukherroub, R.: Biomolecule and nanoparticle transfer on patterned and heterogeneously wetted superhydrophobic silicon nanowire surfaces. *Langmuir* **24**, 1670–1672 (2008)
37. Yan, B., Zhu, Z.-J., Miranda, O.R., Chompoosor, A., Rotello, V.M., Vachet, R.W.: Laser desorption/ionization mass spectrometry analysis of monolayer-protected gold nanoparticles. *Anal. Bioanal. Chem.* **396**, 1025–1035 (2010)
38. Lim, A.Y., Ma, J., Boey, Y.C.F.: Development of nanomaterials for SALDI-MS analysis in forensics. *Adv. Mater.* **24**, 4211–4216 (2012)
39. Pomerantz, A.E., Hammond, M.R., Morrow, A.L., Mullins, O.C., Zare, R.N.: Two-step laser mass spectrometry of asphaltenes. *J. Am. Chem. Soc.* **130**, 7216–7217 (2008)
40. Zare, R.N., Hahn, J.H., Zenobi, R.: Mass-spectrometry of molecular adsorbates using desorption laser multiphoton ionization. *Bull. Chem. Soc. Jpn.* **61**, 87–92 (1988)
41. Engelke, F., Hahn, J.H., Henke, W., Zare, R.N.: Determination of phenylthiohydantoin-amino acids by 2-step laser desorption multiphoton ionization. *Anal. Chem.* **59**, 909–912 (1987)

42. Kovalenko, L.J., Maechling, C.R., Clemett, S.J., Philippoz, J.M., Zare, R.N., Alexander, C.M.O.: Microscopic organic-analysis using 2-step laser mass-spectrometry—application to meteoritic acid residues. *Anal. Chem.* **64**, 682–690 (1992)
43. Hanley, L., Zimmermann, R.: Light and molecular ions: The emergence of vacuum UV single-photon ionization in MS. *Anal. Chem.* **81**, 4174–4182 (2009)
44. Mahajan, T.B., Plows, F.L., Gillette, J.S., Zare, R.N., Logan, G.A.: Comparison of microprobe two-step laser desorption/laser ionization mass spectrometry and gas chromatography/mass spectrometry studies of polycyclic aromatic hydrocarbons in ancient terrestrial rocks. *J. Am. Soc. Mass Spectrom.* **12**, 989–1001 (2001)
45. Fye, J.L., Nelson, H.H., Mowery, R.L., Baronavski, A.P., Callahan, J.H.: Scanning ultraviolet two-step laser mass spectroscopy of polycyclic aromatic hydrocarbon distributions on creosote-contaminated soil particles. *Anal. Chem.* **74**, 3019–3029 (2002)
46. Gillette, J.S., Luthy, R.G., Clemett, S.J., Zare, R.N.: Direct observation of polycyclic aromatic hydrocarbons on geosorbents at the subparticle scale. *Environ. Sci. Technol.* **33**, 1185–1192 (1999)
47. Plows, F.L., Elsila, J.E., Zare, R.N., Buseck, P.R.: Evidence that polycyclic aromatic hydrocarbons in two carbonaceous chondrites predate parent-body formation. *Geochim. Cosmochim. Acta* **67**, 1429–1436 (2003)
48. Spencer, M.K., Hammond, M.R., Zare, R.N.: Laser mass spectrometric detection of extraterrestrial aromatic molecules: Mini-review and examination of pulsed heating effects. *Proc. Natl. Acad. Sci. U. S. A.* **105**, 18096–18101 (2008)
49. Clemett, S.J., Maechling, C.R., Zare, R.N., Swan, P.D., Walker, R.M.: Identification of complex aromatic-molecules in individual interplanetary dust particles. *Science* **262**, 721–725 (1993)
50. Greenberg, J.M., Gillette, J.S., Caro, G.M.M., Mahajan, T.B., Zare, R.N., Li, A.G., Schutte, W.A., de Groot, M., Mendoza-Gomez, C.: Ultraviolet photoprocessing of interstellar dust mantles as a source of polycyclic aromatic hydrocarbons and other conjugated molecules. *Astrophys. J.* **531**, L71–L73 (2000)
51. Spencer, M.K., Clemett, S.J., Sandford, S.A., McKay, D.S., Zare, R.N.: Organic compound alteration during hypervelocity collection of carbonaceous materials in aerogel. *Meteorit. Planet. Sci.* **44**, 15–24 (2009)
52. Haefliger, O.P., Bucheli, T.D., Zenobi, R.: Development of aromatic compounds of urban aerosols in the course of a 24-hour period—a study using two-step laser mass spectrometry. *Analusis* **27**, 337–340 (1999)
53. Orea, J.M., Montero, C., Jimenez, J.B., Urena, A.G.: Analysis of trans-resveratrol by laser desorption coupled with resonant ionization spectrometry. Application to trans-resveratrol content in vine leaves and grape skin. *Anal. Chem.* **73**, 5921–5929 (2001)
54. Zhan, Q., Zenobi, R., Wright, S.J., LangridgeSmith, P.R.R.: Spatially resolved in-situ analysis of polymer additives by two-step laser mass spectrometry. *Macromolecules* **29**, 7865–7871 (1996)
55. Sabbah, H., Morrow, A.L., Pomerantz, A.E., Mullins, O.C., Tan, X., Gray, M.R., Azyat, K., Tykwinski, R.R., Zare, R.N.: Comparing laser desorption/laser ionization mass spectra of asphaltenes and model compounds. *Energy Fuel* **24**, 3589–3594 (2010)
56. Sabbah, H., Pomerantz, A.E., Wagner, M., Muellen, K., Zare, R.N.: Laser desorption single-photon ionization of asphaltenes: Mass range, compound sensitivity, and matrix effects. *Energy Fuel* **26**, 3521–3526 (2012)
57. Bucheli, T.D., Haefliger, O.P., Dietiker, R., Zenobi, R.: Analysis of water contaminants and natural water samples using two-step laser mass spectrometry. *Anal. Chem.* **72**, 3671–3677 (2000)
58. Sabbah, H., Morrow, A.L., Jenniskens, P., Shaddad, M.H., Zare, R.N.: Polycyclic aromatic hydrocarbons in asteroid 2008 TC3: Dispersion of organic compounds inside asteroids. *Meteorit. Planet. Sci.* **45**, 1710–1717 (2010)
59. Hahn, J.H., Zenobi, R., Zare, R.N.: Subfemtomole quantitation of molecular adsorbates by 2-step laser mass-spectrometry. *J. Am. Chem. Soc.* **109**, 2842–2843 (1987)
60. Elsila, J.E., de Leon, N.P., Zare, R.N.: Factors affecting quantitative analysis in laser desorption/laser ionization mass spectrometry. *Anal. Chem.* **76**, 2430–2437 (2004)
61. Acevedo, S., Gutierrez, L., Negrin, G., Pereira, J.C., Mendez, B., Delolme, F., Dessalces, G., Broseta, D.: Molecular weight of petroleum asphaltenes: A comparison between mass spectrometry and vapor pressure osmometry. *Energy Fuel* **19**, 1548–1560 (2005)
62. Tanaka, R., Sato, S., Takanohashi, T., Hunt, J.E., Winans, R.E.: Analysis of the molecular weight distribution of petroleum asphaltenes using laser desorption-mass spectrometry. *Energy Fuel* **18**, 1405–1413 (2004)
63. Al-Muhareb, E., Morgan, T.J., Herod, A.A., Kandiyoti, R.: Characterization of petroleum asphaltenes by size exclusion chromatography, UV-fluorescence and mass spectrometry. *Pet. Sci. Technol.* **25**, 81–91 (2007)
64. Mullins, O.C., Sabbah, H., Eyssautier, J., Pomerantz, A.E., Barre, L., Andrews, A.B., Ruiz-Morales, Y., Mostowfi, F., McFarlane, R., Goual, L., Lepkowicz, R., Cooper, T., Orbulescu, J., Leblanc, R.M., Edwards, J., Zare, R.N.: Advances in asphaltene science and the Yen–Mullins model. *Energy Fuel* **26**, 3986–4003 (2012)
65. Mullins, O.C.: The modified Yen model. *Energy Fuel* **24**, 2179–2207 (2010)